Genes involved in osteogenic differentiation induced by low-intensity pulsed ultrasound in goldfish scales

YOSHIAKI TABUCHI[1], KOUHEI KURODA[2], YUKIHIRO FURUSAWA[3], TETSUSHI HIRANO[1], RYO NAGAOKA[4], MASAAKI OMURA[4], HIDEYUKI HASEGAWA[4], JUN HIRAYAMA[5] and NOBUO SUZUKI[2]

[1]Division of Molecular Genetics Research, Life Science Research Center, University of Toyama, Toyama 930-0194, Japan; [2]Noto Marine Laboratory, Institute of Nature and Environmental Technology, Kanazawa University, Ishikawa 927-0553, Japan; [3]Department of Pharmaceutical Engineering, Faculty of Engineering, Toyama Prefectural University, Toyama 939-0398, Japan; [4]Laboratory of Medical Information Sensing, Faculty of Engineering, University of Toyama, Toyama 930-8555, Japan; [5]Department of Clinical Engineering, Faculty of Health Sciences, Komatsu University, Ishikawa 923-0961, Japan

Received April 2, 2024; Accepted July 9, 2024

DOI: 10.3892/br.2024.1896

Abstract. The teleost scale is a unique calcified tissue that contains osteoclasts, osteoblasts, osteocytes and the bone matrix, similar to mammalian bone. Here, the effects of low-intensity pulsed ultrasound (LIPUS) on osteoblasts and osteoclasts in goldfish scales were investigated. Scales were treated with LIPUS, which is equivalent to use under clinical conditions (30 mW/cm^2 for 20 min), then cultured at 15˚C. Alkaline phosphatase activity, a marker of osteoblasts, or tartrate-resistant acid phosphatase (TRAP) activity, a marker of osteoclasts was measured. The gene expression profile was examined using RNA-sequencing. Gene network and biological function analyses were performed using the Ingenuity® Pathways Knowledge Base. A single exposure of LIPUS significantly increased ALP activity but did not affect TRAP activity. These data indicated that LIPUS induced osteoblastic activation in goldfish scales. Using RNA-sequencing, numerous genes that were significantly and differentially expressed 3, 6, and 24 h after LIPUS exposure were observed. Ingenuity® pathway analysis demonstrated that three gene networks, GN-3h, GN-6h, and GN-24h, were obtained from upregulated genes at 3, 6 and 24 h culture, respectively, and included several genes associated with osteoblast differentiation, such as protein kinase D1, prostaglandin-endoperoxide synthase 2, TNFRSF11B (tumor necrosis factor receptor superfamily, member 11b) and WNT3A (Wnt family member 3A). A significant upregulation of expression levels of these genes in scales treated with LIPUS was confirmed by reverse transcription-quantitative polymerase chain reaction. These results contribute to elucidating the molecular mechanisms of osteoblast activation induced by LIPUS.

Correspondence to: Professor Yoshiaki Tabuchi, Division of Molecular Genetics Research, Life Science Research Center, University of Toyama, 2630 Sugitani, Toyama 930-0194, Japan
E-mail: ytabu@cts.u-toyama.ac.jp

Abbreviations: ADRB2, adrenoceptor β2; ALP, alkaline phosphatase; COX-2, cyclooxygenase 2; DEG, differentially expressed gene; HSP90AA1, heat shock protein 90α family class A member 1; LIPUS, low-intensity pulsed ultrasound; OPG, osteoprotegerin; PGE2, prostaglandin E2; PRKD1, protein kinase D1; PTGS2, prostaglandin-endoperoxide synthase 2; RNA-seq, RNA-sequencing; RT, reverse transcription; TNFRSF11B, tumor necrosis factor receptor superfamily, member 11b; TPM, transcripts per million reads; TRAP, tartrate-resistant acid phosphatase

Key words: low-intensity pulsed ultrasound, goldfish scale, alkaline phosphatase activity, gene expression

Introduction

Ultrasound (US) is a sound wave with frequencies >20 kHz and has been widely used in diagnosis and therapy in medicine (1-6). Acoustic intensities for diagnosis are typically <100 mW/cm^2 (1-3). In cancer therapy, high-intensity focused ultrasound is used (5,6). For example, the acoustic intensity used for prostate cancer ranges from 100 to 10,000 mW/cm^2 spatial average-temporal average intensity (I_{SATA}) (6). Low-intensity pulsed US (LIPUS) is a well-recognized non-invasive therapy and has garnered attention as a potential adjunctive therapy for accelerating bone fracture healing (3,4). LIPUS clinical protocol for fractures involves a 1.5 MHz sine wave repeated at 1 kHz at 30 mW/cm^2 I_{SATA} with a pulsed width of 200 μsec for 20 min/day (3,4). LIPUS has been shown to augment bone fracture healing in experimental animal models, using rabbits (7), rats (8,9) and mice (10), as well as clinical settings (11,12). Although molecular mechanisms underlying the effects of LIPUS remain poorly elucidated, numerous *in vitro* studies have demonstrated positive osteogenic effects of LIPUS on bone cells during fracture healing (13-21).

Mammalian bone is an active mineralized connective tissue composed of three types of cell: Osteoblasts, osteoclasts and osteocytes (22). Mechanical loading has also been widely recognized as an essential factor for the maintenance of bone.

It is well known that both bone matrix and osteocytes play an important role in sensing mechanical loading of bone (23-25). Similarly, the teleost scale is a unique calcified tissue in which osteoclasts, osteoblasts and two layers of the bone matrix are present (26-28). Furthermore, our previous study demonstrated the existence of osteocyte-like cells in goldfish scales (29). Fish scales are therefore a suitable model for bone mechanotransduction, the conversion of mechanical stimulus into a biological response. Osteoblasts and osteoclasts in goldfish scales respond sensitively to mechanical loading such as hypergravity (27), microgravity (30) and ultrasound (16,31,32).

RNA-sequencing (RNA-seq) using next-generation sequencing (NGS) technology is a powerful tool that applies genome-wide expression profiles to a wider range of organisms, even in non-model organisms with no established databases, compared with DNA microarray (33). Our previous studies reported that melatonin suppresses osteoclast activation and cell damage induced by space flight in goldfish scales using RNA-seq method (30,34). The present study examined the effects of LIPUS (30 mW/cm^2) on the osteoblasts and osteoclasts of goldfish scales and performed global-scale gene expression analysis of scales treated with LIPUS using RNA-seq to determine the underlying mechanism.

Materials and methods

Animals and preparation of fish scales. Goldfish (Carassius auratus) were obtained from Higashikawa Fish Farm (Yamatokoriyama, Japan). A total of 12 male fish (weight, 30-40 g; age, ~2 years) were fed a commercial pellet diet (Spectrum Brands Japan) every morning and were maintained in freshwater (pH, 7.0-7.5) at 26˚C under a 12 h light/12 h dark cycle (32). All experimental procedures were conducted in accordance with the Guide for Care and Use of Laboratory Animals and approved by Animal Research Committee of Kanazawa University (approval no. 242-2023) and were performed under anesthesia to minimize pain. In addition, all experimental protocols were in strict accordance with the ARRIVE guidelines 2.0 (35).

Regenerating scales that had active osteoclasts and osteoblasts were used for analysis of LIPUS treatments (27). In brief, goldfish were anesthetized in freshwater containing ethyl 3-aminobenzoate methanesulfonic acid salt (MS-222; 330 mg/l; Sigma-Aldrich; Merck KGaA) (34). Adequate anesthesia was indicated cessation of opercular movements. The normal scales that developed on the body were removed to allow the regeneration of scales under anesthesia. The anesthetized fish were returned to freshwater, allowed to recover and the goldfish were maintained as aforementioned. Behavior and feeding activity were monitored daily to check health. At 14 days after the removal of normal scales, regenerating scales were removed from the goldfish under anesthesia and were placed in a 6-well cell culture plate (Nippon Genetics, Co., Ltd.) with 2 ml Leibovitz's L-15 medium (Invitrogen; Thermo Fisher Scientific, Inc.) containing 1% penicillin-streptomycin mixture (ICN Biomedicals, Inc.) and incubated for 2 h at 15˚C before use (27,32). Goldfish were anesthetized using MS-222. Once opercular movements ceased, anesthesia was continued for an additional 40 min to euthanize the goldfish. The goldfish, which were no longer responding to stimuli and not moving, were then returned to freshwater. Death was confirmed following no recovery within 20 min.

LIPUS treatment and temperature measurement of culture medium. LIPUS treatment was applied using an ultrasound irradiating system in a 6-well cell culture plate (No. US-Vitro-N04-48; Teijin Pharma, Ltd.; Fig. 1) (36). (3,4). The signal had an I_{SATA} of 30 mW/cm^2, with a frequency of 1.5 MHz in a pulsed-wave mode (0.2-sec burst sine waves repeated at 1.0 kHz). When the scales were treated with LIPUS, the 6-well cell culture plate containing scales was placed on the transducer. LIPUS was transmitted through the bottom of the cell culture plate. The scales were irradiated with LIPUS for 20 min at room temperature. For control group, the scales were incubated for 20 min without LIPUS treatment in the aforementioned LIPUS-exposure setup as described above. The treated scales were further incubation for 3, 6 or 24 h at 15˚C.

The biophysical effects of ultrasound on living tissue are divided into thermal and non-thermal effects (2). Temperature of the culture medium was monitored with a digital thermometer coupled to a type K thermocouple sensor (Sato Keiryoki MFG Co., Ltd.) at room temperature (37).

Assay of alkaline phosphatase (ALP) and tartrate-resistant acid phosphatase (TRAP) activity. ALP or TRAP activity was measured using alkaline (1 mM $MgCl_2$ and 100 mM Tris-HCl, pH 9.5) or acidic buffer (100 mM sodium acetate and 20 mM tartrate, pH 5.3), respectively. In short, a 100 μl aliquot of alkaline or acidic buffer was added to each well at room temperature. Then, each scale was placed into a well in a 96-well microplate. This microplate was immediately frozen at -80˚C and then kept at -20˚C until analysis. A 100 μl aliquot of 20 mM para-nitrophenyl (pNP) phosphate in alkaline or acidic buffer was added to each well at room temperature. The plate was incubated at 23˚C for 20 min with shaking. The reaction was stopped by adding 50 μl 3 M NaOH. A total of 150 μl reacted solution was transferred to a new plate and the absorbance was measured at 405 nm. The absorbance was converted into the amount of pNP produced using a standard curve. After measuring both ALP and TRAP activity, the scales were measured with Image J software (Ver. 1.53; https://imagej.net/ij/index.html). ALP and TRAP activities were normalized to the surface area (mm^2) of each scale (27).

RNA isolation. Total RNA was isolated from the regenerating scales of goldfish using RNeasy Fibrous Tissue Mini kit (cat. no. 74704; Qiagen GmbH). The concentration of RNA was measured by spectroscopy with an expected A260/A280 ratio close to 2. RNA quality was analyzed using a Bioanalyzer 2100 and RNA 6000 Nano kit (Cat. No. 5067-1511; Agilent Technologies, Inc.). Total RNA with RNA integrity number >9.0 was used for RNA-seq and reverse transcription-quantitative (RT-q)PCR.

RNA-seq, gene expression and gene network analyses. RNA-seq was performed by Veritas Genetics Co. The analysis was conducted with the Novaseq6000 sequencer (Illumina, Inc.), and data of nucleotide length 150 bp (directional paired-end reads) was provided.

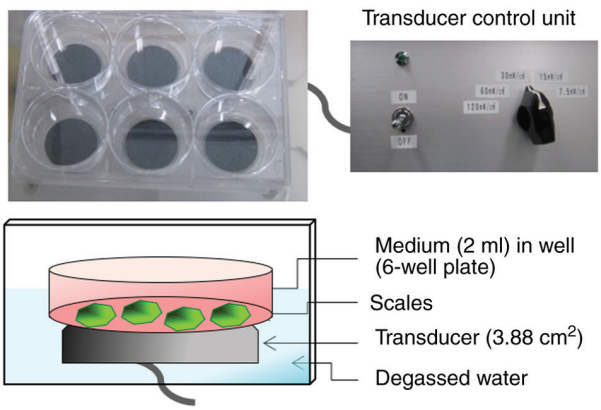

Figure 1. Schematic illustration of the low-intensity pulsed ultrasound irradiation system.

Quality check of raw read sequences was performed using FastQC (Ver. 0.11.8; http://www.bioinformatics.babraham.ac.uk/projects/fastqc). Adaptors and short, low-quality reads (Q<20; <50 bp) were trimmed using TrimGalore (Ver. 1.18; bioinformatics.babraham.ac.uk/projects/trim_galore/). For *de novo* transcriptome assembly and read mapping, following PCR duplicate removal using seqkit (38), *de novo* transcriptome assembly of processed reads was performed using Trinity (r2012-10-05; cell-innovation.nig.ac.jp/index_en.html) was used with default parameters to generate a reference sequence of transcripts (33). To estimate relative RNA expression levels as transcripts per million reads (TPM), sequence reads with PCR duplicates were pseudo-mapped to the reference sequence of transcripts using Kallisto with strict parameters (k-mer size: 31; bootstrap-samples: 0; min-size: automatically chosen; ec-max-size: no maximum) (39). To normalize gene expression, statistical analysis of TPM was performed using Strand NGS v3.3 with the Trimmed Mean of M value (TMM) (40). TMM is a normalized method that is generally used for analyzing omics data (https://genomebiology.biomedcentral.com/articles/10.1186/gb-2010-11-3-r25). Furthermore, differentially expressed genes (DEGs) in LIPUS, compared with LIPUS non-treated scales, were identified using unpaired t-test and multiple testing Benjamini-Hochberg correction. Genes were considered differentially expressed when P<0.05 and fold-change ≥1.2. The obtained data were analyzed using Ingenuity® Pathway Analysis tools (Qiagen GmbH) to examine Gene Ontology (geneontology.org/) enrichment, including biological processes, cellular components, molecular functions, and gene networks. Upregulated genes at 3, 6 and 24 h after LIPUS treatment were uploaded to the Ingenuity® Pathway Analysis tools. Core analysis was performed, followed by analysis of biological functions, especially osteoblastic differentiation. Candidate genes were analyzed using Gene Network Analysis to generate gene networks based on known interactions (37,41).

RT-qPCR. Complementary DNA was produced from total RNA using a PrimeScript™ RT kit with gDNA Eraser (Takara Bio, Inc.) according to the manufacturer's protocol. RT-qPCR was performed on an Mx3005P real-time PCR system (Agilent Technologies, Inc.) using SYBR® Premix Ex Taq™ II (Tli RNaseH Plus; Takara Bio, Inc.). The specific primer sequences are listed in Table I. The thermocycling conditions were as follows: Initial denaturation for 10 min at 95˚C, followed by 40 cycles of 10 sec at 95˚C and 40 sec at 60˚C. For quantification, the standard curve method was used (42). Moreover, PCR products were electrophoresed through a 2% agarose gel at 100 V for 30 min using the Mupid-2plus gel electrophoresis system (Takara Bio Inc.) After staining with ethidium bromide (0.5 μg/ml) for 15 min at room temperature, gel bands were visualized using a gel imaging system (Printgraph TYPE-GX, ATTO Co.). β-actin was used as an internal control (37,43).

Table I. Nucleotide sequences of primers for target genes.

Gene	Sequence, 5'→3'
ACTB	F: TGTGCTGTCCCTGTATGCCT
	R: ATTTCCCTCTCGGCTGTGGT
PRKD1	F: GCCATTCTCCAGAACCTC
	R: AGAAACTTGGTGATGCGT
PTGS2	F: TGTGTTCGGGGAGACTATGG
	R: CCACTTTCCCACCAAACGTG
TNFRSF11B	F: TGACAGGTGTCCTCCAGGAA
	R: TCCAGAACTCCGTGAACAGAC
WNT3A	F: ACCGAAACTGACCTGGTCTAC
	R: CAAGTCGCAGCCATCGATAC

F, forward; R, reverse; ACTB, β-actin; PRKD1, protein kinase D1; PTGS2, prostaglandin-endoperoxide synthase 2; TNFRSF11B, tumor necrosis factor receptor superfamily, member 11b; WNT3A, Wnt family member 3A.

Statistical analysis. Data are presented as the mean ± SD of three or more independent experiments. The values of the control scales were compared with those of LIPUS-treated scales. Differences were analyzed using a paired t test. Statistical analysis was performed using R software (Ver. 4.3.3.; r-project.org/). P<0.05 was considered to indicate a statistically significant difference.

Results

Effect of LIPUS on temperature of culture medium. Biophysical effects of ultrasound on living tissues are divided into thermal and nonthermal effects (2). Therefore, the effects of LIPUS on the temperature of the culture medium were determined. The initial temperature of the culture medium was 24.9±0.2˚C. The temperature of the culture medium 20 min after LIPUS treatment was not significantly increased (25.0±0.2˚C), suggesting thermal effects were not included in the bioeffects of LIPUS.

Effects of LIPUS on ALP and TRAP activity of goldfish scales. LIPUS treatment significantly increased ALP activity, a marker of osteoblasts, but did not affect TRAP activity, a marker of osteoclasts (Fig. 2A). These data indicated that LIPUS induced osteoblastic activation in goldfish scales.

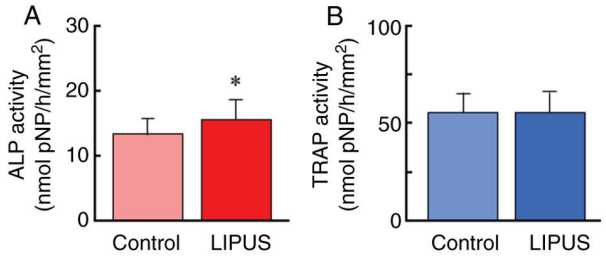

Figure 2. Effect of LIPUS on ALP and TRAP activity. Goldfish scales were irradiated with LIPUS at 30 mW/cm^2 for 20 min, then cultured at 15˚C for 24 h. (A) ALP and (B) TRAP activity was measured. *P<0.05 vs. control. LIPUS, low-intensity pulsed ultrasound; ALP, alkaline phosphatase; TRAP, tartrate-resistant acid phosphatase; pNP, para-nitrophenol.

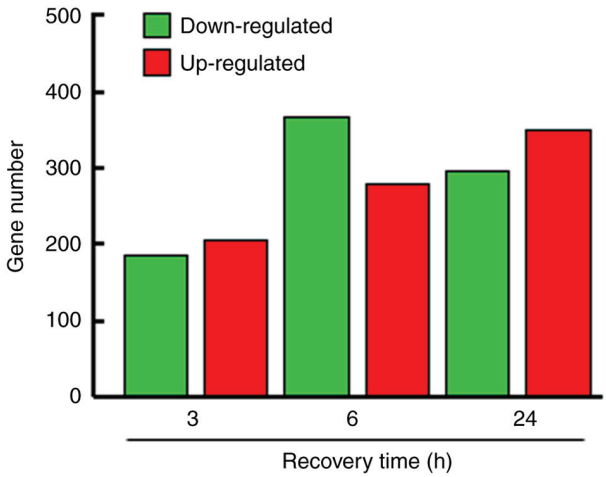

Figure 3. DEGs induced by LIPUS treatment. Goldfish scales were irradiated with LIPUS at 30 mW/cm^2 for 20 min, then cultured at 15˚C for 3, 6 and 24 h. RNA sequencing analysis was performed. The number of DEGs with P<0.05 and fold-change ≥1.2 is shown. DEG, differentially expressed gene; LIPUS, low-intensity pulsed ultrasound.

Gene expression analysis. To identify candidate genes responsive to LIPUS treatment, the time course of the gene expression profile was examined using RNA-seq. Gene expression analysis of the scales exposed to LIPUS revealed 207, 280 and 350 upregulated genes at 3, 6 and 24 h, respectively, and 188, 368 and or 298 downregulated genes at 3, 6 and 24 h, respectively (Fig. 3). The complete lists of DEGs from the goldfish scale samples are shown in Tables SI-SVI.

Gene network and biological function analysis. To examine the functional association between candidate genes, gene network and biological function analyses were performed using the Ingenuity® Pathways Knowledge Base. Significant gene networks, GN-3h, GN-6h and GN-24h, were identified from upregulated genes at 3, 6 and 24 h after LIPUS treatment, respectively (Fig. 4). GN-3h consisted of nine genes: Adrenoceptor β2 (ADRB2), BAG cochaperone 3, heat shock protein 90α family class A member 1 (HSP90AA1), MAPK11, MET proto-oncogene, receptor tyrosine kinase, protein kinase D1 (PRKD1), Rho-related BTB domain containing 1, receptor tyrosine kinase-like orphan receptor 1 and tumor necrosis factor receptor superfamily, member 11b (TNFRSF11B) (Fig. 4A). GN-6h consisted of six genes: Aryl hydrocarbon receptor repressor, cytochrome P450 family 1 subfamily A member 1, DEP domain-containing 1B, OTU deubiquitinase with linear linkage specificity, TNFRSF11B and Wnt family member 3A (WNT3A; Fig. 4B). GN-24h consisted of seven genes: Caspase 9, fibrillarin, granzyme B, prostaglandin-endoperoxide synthase 2 (PTGS2), TATA box-binding protein-associated factor 15, transducin β-like 3 and transglutaminase 1 (Fig. 4C). ADRB2, MAPK11, PRKD1, PTGS2, TNFRSF11B and WNT3A were associated with biological functions of osteogenesis, including osteoblast differentiation and bone development and formation.

Effects of LIPUS on gene expression. PRKD1, TNFRSF11B, WNT3A and PTGS2–were selected from the three gene networks. The specificity of the primers was confirmed by a single band with the correctly amplified fragment size through agarose gel electrophoresis of the PCR products (Supplementary material Fig. S1). Expression of PRKD1 was significantly upregulated at 3 h and TNFRSF11B was significantly upregulated at all time points (Fig. 5A and B). The expression of WNT3A was significantly upregulated at 6 h and PTGS2 was significantly upregulated at 3 and 24 h after LIPUS treatment (Fig. 5C and D). These data were comparable with the RNA-seq results.

Discussion

Numerous studies have shown that LIPUS induces osteogenic activity in *in vitro* experimental models (13-21). For example, ALP activity, a marker of osteoblasts, in mouse preosteoblast MC3T3-E1 (14) and bone marrow mesenchymal stem cells (21) is significantly increased in response to clinical application of LIPUS (30 mW/cm^2 for 20 min). Kitamura *et al* (16) demonstrated that LIPUS at 60 mW/cm^2 for 6-20 min significantly elevates ALP activity in goldfish scales. In agreement with previous studies (14,16,21), here, LIPUS (30 mW/cm^2 for 20 min) significantly increased ALP activity but did not affect TRAP activity, a marker of osteoclasts, suggesting that LIPUS induced osteoblastic activation in goldfish scales. On the other hand, in our previous study, the same clinical LIPUS application affected osteoclasts in fish scales; LIPUS directly caused apoptosis in osteoclasts 3 h after treatment in both zebrafish and goldfish scales (31) and moderately activated osteoclasts 6 and 12 h after treatment in goldfish scales (32). LIPUS was transmitted through the bottom of the cell culture plate or directly from the upper side in the present osteoblast-activating or previous osteoclast-affecting conditions (31,32), respectively. The discrepancy in the effects of LIPUS between the present and previous studies may have been related to this difference in the LIPUS-exposure conditions. In addition, 2 weeks after daily LIPUS treatment, ALP activity and regeneration rate are significantly increased in goldfish scales *in vivo* (32). The present results and those of previous studies (16,31,32) suggest that osteoblasts and osteoclasts in fish scales respond sensitively to LIPUS mechanical stress.

The present study used RNA-seq and Ingenuity® pathway analyses to identify DEGs and three unique gene networks. These networks included ADRB2, MAPK11, PRKD1, TNFRSF11B, WNT3A and PTGS2, which are known to be involved in various aspects of osteogenesis, including osteoblast

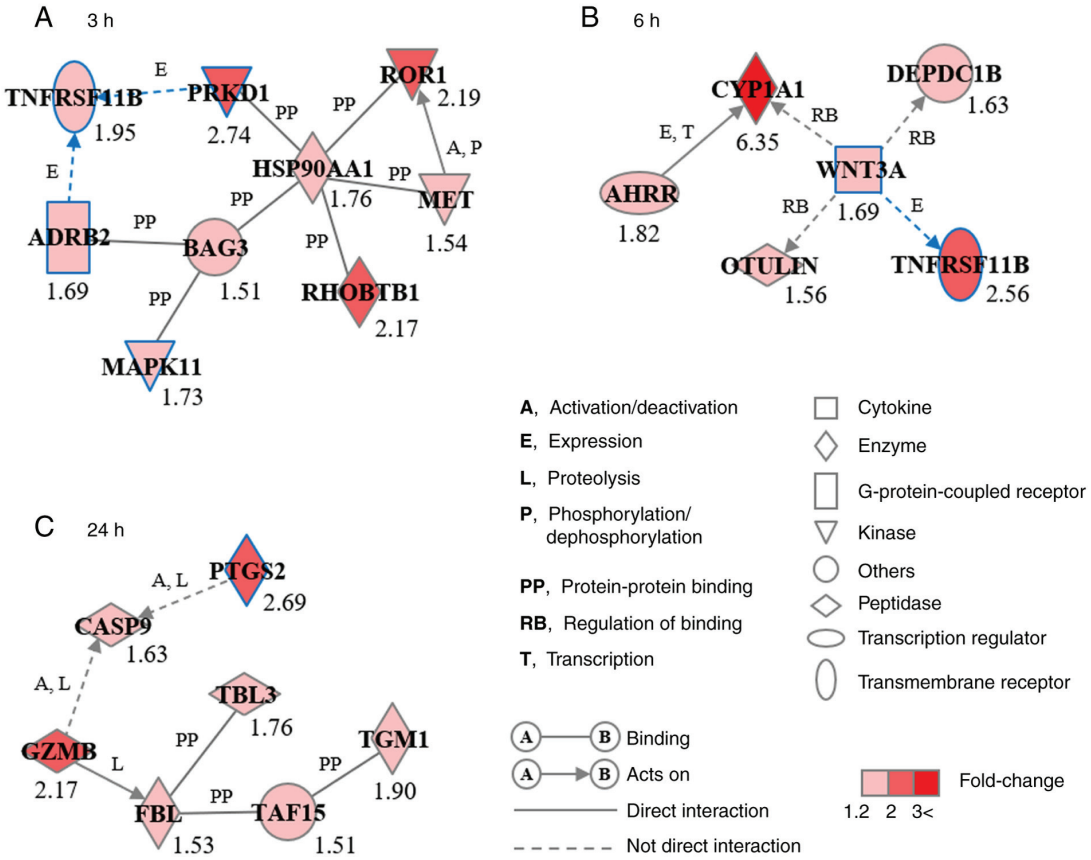

Figure 4. Upregulated genes in scales treated with low-intensity pulsed ultrasound after 3, 6, and 24 h were analyzed using the Ingenuity® Pathway Analysis tools. Gene networks were identified from upregulated genes at (A) 3, (B) 6 and (C) 24 h. Blue, biological functions of osteogenesis, including osteoblast differentiation and bone development and formation.

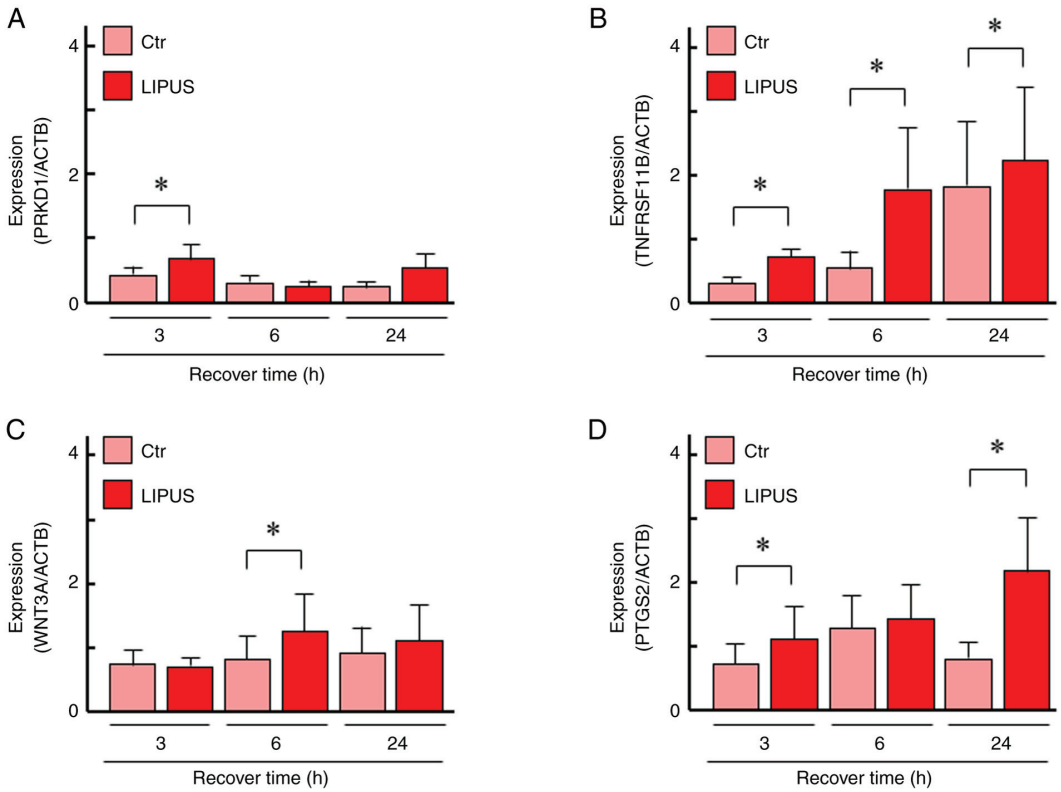

Figure 5. Effects of LIPUS on the gene expression. Gene expression levels of (A) PRKD1, (B) TNFRSF11B, (C) WNT3A and (D) PTGS2 were normalized to ACTB. *P<0.05 vs. Ctr. ACTB, β-actin; PRKD1, protein kinase D1; TNFRSF11B, tumor necrosis factor receptor superfamily, member 11b; WNT3A, Wnt family member 3A; PTGS2, prostaglandin-endoperoxide synthase 2; Ctr, control.

differentiation and bone development and formation (44-53). Previous research using knockout mice demonstrated that ADRB2 (44) and PRKD1 (45) are key to bone formation, while TNFRSF11B (46) and MAPK11 (47) serve key roles in bone development. PRKD1 (48), TNFRSF11B (49), WNT3A (50) and PTGS2 (51) induce osteoblast differentiation in experimental models such as MC3T3-E1 mouse preosteoblastic cells (48,49), C2C12 (48) and C3H10T1/2 (50) mouse mesenchymal stem cells, as well as PTGS2 knockout mice (51). Interactions have been reported between TNFRSF11B and ADRB2 (44), PRKD1 (52) and WNT3A (53).

The product translated from TNFRSF11B, known as osteoprotegerin (OPG) and produced by osteoblasts, functions as a decoy receptor of receptor activator for nuclear factor-κB ligand (RANKL) and suppresses osteoclastogenesis (54). One of the most effective approaches for clinically treating osteoporosis involves the use of a specific antibody to inhibit RANKL, a mechanism akin to that of OPG (55). Yu *et al* (49) indicated that ALP activity is significantly higher in the OPG-overexpressing preosteoblast cell line MC3T3-E1, indicating that OPG promotes matrix maturation in preosteoblasts. Moreover, reports indicate that OPG enhances osteoblastogenesis of human mesenchymal stem cells (18,56) and LIPUS (400 mW/cm^2, 20 min) boosts osteoblastogenesis of human mesenchymal stem cells by increasing mRNA levels of TNFRSF11B and ALP (18). Moreover, Borsje *et al* (15) reported that the clinical application of LIPUS significantly increases OPG mRNA and protein expression in human osteoblast-like Saos-2 cells. Furthermore, *in vivo* study using an ovariectomy-induced osteoporotic fracture rat model found that clinical application of LIPUS accelerates osteoporotic fracture healing. Moreover, OPG gene expression is upregulated in LIPUS-treated rats at an earlier stage of the repair process compared with controls (9). In our previous study using goldfish scales, OPG was suggested to suppress excessive bone resorption under osteoclast-activated conditions induced by clinical application of LIPUS (32). In the present study, LIPUS induced TNFRSF11B expression and ALP activity without interfering with TRAP activity. This suggested that in LIPUS-treated goldfish scales, OPG may be involved in osteoblastic differentiation rather than suppression of osteoclastogenesis.

Cyclooxygenase 2 (COX-2), which is encoded by PTGS2, is a key enzyme in prostaglandin E2 (PGE2) biosynthesis. LIPUS stimulation increases expression of PTGS2 and PGE2 in bone cells (13,37,57-59). Tang *et al* (13) demonstrated that the clinical application of LIPUS stimulates mineralization of osteoblasts via the COX-2/PGE2 pathway. COX-2 and PGE2 are reported to play essential roles in the regulation of osteoblastic differentiation (13,51,60) and fracture healing (3,4,10). Naruse *et al* (10) used knockout mice to demonstrate that LIPUS accelerates endochondral bone healing during senescence in a COX-2-dependent manner. A delay in fracture healing is also observed in rats and humans administered COX inhibitors (61,62). In the present study, expression of *PTGS2* was elevated 24 h after LIPUS treatment in goldfish scales. Omori *et al* (63) demonstrated that the addition of PGE2 to goldfish scales promotes both osteoblastic and osteoclastic activity. The present data along with the previous findings suggest that LIPUS stimulation may enhance osteoblastogenesis via the COX-2/PGE2 pathway. Investigating the effects of LIPUS on osteoblastgenesis in goldfish scales treated with either COX-2 inhibitor or small interfering RNA for PTGS2 is required.

Hsp90α, the product of HSP90AA1, belongs to the HSP family and exhibits potent chaperone activity (64). This protein is induced by stressors, including heat stress, and is mediated primarily by heat shock transcription factor 1 (65). In the present study, expression of HSP90AA1 was significantly upregulated in the goldfish scales treated with LIPUS, without any temperature rise in the culture medium. This suggested that temperature had little involvement in LIPUS-induced HSP90AA1 expression. Similarly, LIPUS induces HSP90AA1 expression in zebrafish scales (31). Previous studies have also indicated that LIPUS at 30 mW/cm^2 for 15 or 30 min enhances osteogenic differentiation by elevating HSP90AA1 levels in mouse calvaria-derived osteoblasts (19) and human adipose-derived stem cells (20).

Taken together, the present results provide insight into the molecular mechanisms underlying LIPUS-induced osteoblast activation. However, the present study did not conduct morphological evaluations of the LIPUS-treated goldfish scales. The biological and morphological roles of genes and their interactions in LIPUS-treated goldfish scales require further investigation.

Acknowledgements

The authors would like to thank Dr Hidetada Ohnishi (Teijin Pharma, Ltd.) for lending ultrasound irradiating system.

Funding

The present study was supported in part by Japan Society for the Promotion of Science KAKENHI (grant nos. JP17K01353, JP20K12619, JP23K11802 and JP23K10933).

Availability of data and materials

The data generated in the present study may be found in the DNA Data Bank of Japan under accession number PRJDB17555 or at the following URL: ddbj.nig.ac.jp/resource/bioproject/PRJDB17555.

Authors' contributions

YT, YF and NS designed the experiments and wrote the manuscript. YT, KK, YF, TH, RN, MO, HH, JH and NS performed experiments. YT, KK, YF and NS analyzed the data. YT and NS confirm the authenticity of all the raw data. All authors have read and approved the final manuscript.

Ethics approval and consent to participate

All animal experiments were approved by the Animal Research Committee of Kanazawa University (Kanazawa, Japan (approval no. 242-2023).

Patient consent for publication

Not applicable.

Competing interests

The authors declare that they have no competing interests.

References

1. Barnett SB, Ter Haar GR, Ziskin MC, Rott HD, Duck FA and Maeda K: International recommendations and guidelines for the safe use of diagnostic ultrasound in medicine. Ultrasound Med Biol 26: 355-366, 2000.
2. Snehota M, Vachutka J, Ter Haar G, Dolezal L and Kolarova H: Therapeutic ultrasound experiments in vitro: Review of factors influencing outcomes and reproducibility. Ultrasonics 107: 106167, 2020.
3. Padilla F, Puts R, Vico L and Raum K: Stimulation of bone repair with ultrasound: A review of the possible mechanic effects. Ultrasonics 54: 1125-1145, 2014.
4. Harrison A, Lin S, Pounder N and Mikuni-Takagaki Y: Mode & mechanism of low intensity pulsed ultrasound (LIPUS) in fracture repair. Ultrasonics 70: 45-52, 2016.
5. Kennedy JE: High-intensity focused ultrasound in the treatment of solid tumours. Nat Rev Cancer 5: 321-327, 2005.
6. Uchida T, Nakano M, Hongo S, Shoji S, Nagata Y, Satoh T, Baba S, Usui Y and Terachi T: High-intensity focused ultrasound therapy for prostate cancer. Int J Urol 19: 187-201, 2012.
7. Duarte LR: The stimulation of bone growth by ultrasound. Arch Orthop Trauma Surg (1978) 101: 153-159, 1983.
8. Azuma Y, Ito M, Harada Y, Takagi H, Ohta T and Jingushi S: Low-intensity pulsed ultrasound accelerates rat femoral fracture healing by acting on the various cellular reactions in the fracture callus. J Bone Miner Res 16: 671-680, 2001.
9. Cheung WH, Chow SK, Sun MH, Qin L and Leung KS: Low-intensity pulsed ultrasound accelerated callus formation, angiogenesis and callus remodeling in osteoporotic fracture healing. Ultrasound Med Biol 37: 231-238, 2011.
10. Naruse K, Sekiya H, Harada Y, Iwabuchi S, Kozai Y, Kawamata R, Kashima I, Uchida K, Urabe K, Seto K, *et al*: Prolonged endochondral bone healing in senescence is shortened by low-intensity pulsed ultrasound in a manner dependent on COX-2. Ultrasound Med Biol 36: 1098-1108, 2010.
11. Heckman JD, Ryaby JP, McCabe J, Frey JJ and Kilcoyne RF: Acceleration of tibial fracture-healing by non-invasive, low-intensity pulsed ultrasound. J Bone Joint Surg Am 76: 26-34, 1994.
12. Kristiansen TK, Ryaby JP, McCabe J, Frey JJ and Roe LR: Accelerated healing of distal radial fractures with the use of specific, low-intensity ultrasound. A multicenter, prospective, randomized, double-blind, placebo-controlled study. J Bone Joint Surg Am 79: 961-973, 1997.
13. Tang CH, Yang RS, Huang TH, Lu DY, Chuang WJ, Huang TF and Fu WM: Ultrasound stimulates cyclooxygenase-2 expression and increases bone formation through integrin, focal adhesion kinase, phosphatidylinositol 3-kinase, and Akt pathway in osteoblasts. Mol Pharmacol 69: 2047-2057, 2006.
14. Unsworth J, Kaneez S, Harris S, Ridgway J, Fenwick S, Chenery D and Harrison A: Pulsed low intensity ultrasound enhances mineralisation in preosteoblast cells. Ultrasound Med Biol 9: 1468-1474, 2007.
15. Borsje MA, Ren Y, de Haan-Visser HW and Kuijer R: Comparison of low-intensity pulsed ultrasound and pulsed electromagnetic field treatments on OPG and RANKL expression in human osteoblast-like cells. Angle Orthod 80: 498-503, 2010.
16. Kitamura K, Suzuki N, Sato Y, Nemoto T, Ikegame M, Shimizu N, Kondo T, Furusawa Y, Wada S and Hattori A: Osteoblast activity in the goldfish scale responds sensitively to mechanical stress. Comp Biochem Physiol A Mol Integr Physiol 156: 357-363, 2010.
17. Costa V, Carina V, Fontana S, De Luca A, Monteleone F, Pagani S, Sartori M, Setti S, Faldini C, Alessandro R, *et al*: Osteogenic commitment and differentiation of human mesenchymal stem cells by low-intensity pulsed ultrasound stimulation. J Cell Physiol 233: 1558-1573, 2018.
18. Chiu CY, Tsai TL, Vanderby R Jr, Bradica G, Lou SL and Li WJ: Osteoblastogenesis of mesenchymal stem cells in 3-D culture enhanced by low-intensity pulsed ultrasound through soluble receptor activator of nuclear factor kappa B ligand. Ultrasound Med Biol 41: 1842-1852, 2015.
19. Miyasaka M, Nakata H, Hao J, Kim YK, Kasugai S and Kuroda S: Low-intensity pulsed ultrasound stimulation enhances heat-shock protein 90 and mineralized nodule formation in mouse calvaria-derived osteoblasts. Tissue Eng Part A 21: 2829-2839, 2015.
20. Zhang Z, Ma Y, Guo S, He Y, Bai G and Zhang W: Low-intensity pulsed ultrasound stimulation facilitates in vitro osteogenic differentiation of human adipose-derived stem cells via up-regulation of heat shock protein (HSP)70, HSP90, and bone morphogenetic protein (BMP) signaling pathway. Biosci Rep 38: BSR20180087, 2018.
21. Zhou J, Zhu Y, Ai D, Zhou M, Li H, Fu Y and Song J: Low-intensity pulsed ultrasound regulates osteoblast-osteoclast crosstalk via EphrinB2/EphB4 signaling for orthodontic alveolar bone remodeling. Front Bioeng Biotechnol 11: 1192720, 2023.
22. Florencio-Silva R, Sasso GR, Sasso-Cerri E, Simões MJ and Cerri PS: Biology of bone tissue: Structure, function, and factors that influence bone cells. Biomed Res Int 2015: 421746, 2015.
23. Mikuni-Takagaki Y: Mechanical responses and signal transduction pathways in stretched osteocytes. J Bone Miner Metab 17: 57-60, 1999.
24. Klein-Nulend J, Bakker AD, Bacabac RG, Vatsa A and Weinbaum S: Mechanosensation and transduction in osteocytes. Bone 54: 182-190, 2013.
25. Ma Q, Miri Z, Haugen HJ, Moghanian A and Loca D: Significance of mechanical loading in bone fracture healing, bone regeneration, and vascularization. J Tissue Eng 14: 20417314231172573, 2023.
26. Bereiter-Hahn J and Zylberberg L: Regeneration of teleost fish scale. Comp Biochem Physiol 105A: 625-641, 1993.
27. Suzuki N, Kitamura K, Omori K, Nemoto T, Satoh Y, Tabata MJ, Ikegame M, Yamamoto T, Ijiri K, Furusawa Y, *et al*: Response of osteoblasts and osteoclasts in regenerating scales to gravity loading. Biol Sci Space 23: 211-217, 2009.
28. Hirayama J, Hattori A, Takahashi A, Furusawa Y, Tabuchi Y, Shibata M, Nagamatsu A, Yano S, Maruyama Y, Matsubara H, *et al*: Physiological consequences of space flight, including abnormal bone metabolism, space radiation injury, and circadian clock dysregulation: Implications of melatonin use and regulation as a countermeasure. J Pineal Res 74: e12834, 2023.
29. Yamamoto T, Ikegame M, Hirayama J, Kitamura KI, Tabuchi Y, Furusawa Y, Sekiguchi T, Endo M, Mishima H, Seki A, *et al*: Expression of sclerostin in the regenerating scales of goldfish and its increase under microgravity during space flight. Biomed Res 41: 279-288, 2020.
30. Ikegame M, Hattori A, Tabata MJ, Kitamura KI, Tabuchi Y, Furusawa Y, Maruyama Y, Yamamoto T, Sekiguchi T, Matsuoka R, *et al*: Melatonin is a potential drug for the prevention of bone loss during space flight. J Pineal Res 67: e12594, 2019.
31. Suzuki N, Hanmoto T, Yano S, Furusawa Y, Ikegame M, Tabuchi Y, Kondo T, Kitamura K, Endo M, Yamamoto T, *et al*: Low-intensity pulsed ultrasound induces apoptosis in osteoclasts: Fish scales are a suitable model for the analysis of bone metabolism by ultrasound. Comp Biochem Physiol A Mol Integr Physiol 195: 26-31, 2016.
32. Hanmoto T, Tabuchi Y, Ikegame M, Kondo T, Kitamura KI, Endo M, Kobayashi I, Mishima H, Sekiguchi T, Urata M, *et al*: Effects of low-intensity pulsed ultrasound on osteoclasts: Analysis with goldfish scales as a model of bone. Biomed Res 38: 71-77, 2017.
33. Haas BJ, Papanicolaou A, Yassour M, Grabherr M, Blood PD, Bowden J, Couger MB, Eccles D, Li B, Lieber M, *et al*: De novo transcript sequence reconstruction from RNA-seq using the Trinity platform for reference generation and analysis. Nat Protoc 8: 1494-1512, 2013.
34. Furusawa Y, Yamamoto T, Hattori A, Suzuki N, Hirayama J, Sekiguchi T and Tabuchi Y: De novo transcriptome analysis and gene expression profiling of fish scales isolated from Carassius auratus during space flight: Impact of melatonin on gene expression in response to space radiation. Mol Med Rep 22: 2627-2636, 2020.
35. Percie du Sert N, Ahluwalia A, Alam S, Avey MT, Baker M, Browne WJ, Clark A, Cuthill IC, Dirnagl U, Emerson M, *et al*: Reporting animal research: Explanation and elaboration for the ARRIVE guidelines 2.0. PLoS Biol 18: e3000411, 2020.
36. Iwabuchi S, Ito M, Hata J, Chikanishi T, Azuma Y and Haro H: In vitro evaluation of low-intensity pulsed ultrasound in herniated disc resorption. Biomaterials 26: 7104-7114, 2005.

37. Tabuchi Y, Hasegawa H, Suzuki N, Furusawa Y, Hirano T, Nagaoka R, Hirayama J, Hoshi N and Mochizuki T: Genetic response to low-intensity ultrasound on mouse ST2 bone marrow stromal cells. Mol Med Rep 23: 173, 2021.
38. Shen W, Le S, Li Y and Hu F: SeqKit: A cross-platform and ultrafast toolkit for FASTA/Q file manipulation. PLoS One 11: e0163962, 2016.
39. Bray NL, Pimentel H, Melsted P and Pachter L: Near-optimal probabilistic RNA-seq quantification. Nat Biotechnol 34: 525-527, 2016
40. Robinson MD and Oshlack A: A scaling normalization method for differential expression analysis of RNA-seq data. Genome Biol 11: R25, 2010.
41. Tabuchi Y, Takasaki I, Doi T, Ishii Y, Sakai H and Kondo T: Genetic networks responsive to sodium butyrate in colonic epithelial cells. FEBS Lett 580: 3035-3041, 2006.
42. Larionov A, Krause A and Miller W: A standard curve based method for relative real time PCR data processing. BMC Bioinformatics 6: 62, 2005.
43. Tabuchi Y, Ohta S, Arai Y, Kawahara M, Ishibashi K, Sugiyama N, Horiuchi T, Furusawa M, Obinata M, Fuse H, *et al*: Establishment and characterization of a colonic epithelial cell line MCE301 from transgenic mice harboring temperature-sensitive simian virus 40 large T-antigen gene. Cell Struct Funct 25: 297-307, 2000.
44. Hanyu R, Wehbi VL, Hayata T, Moriya S, Feinstein TN, Ezura Y, Nagao M, Saita Y, Hemmi H, Notomi T, *et al*: Anabolic action of parathyroid hormone regulated by the β2-adrenergic receptor. Proc Natl Acad Sci USA 109: 7433-7438, 2012.
45. Bollag WB, Choudhary V, Zhong Q, Ding KH, Xu J, Elsayed R, Yu K, Su Y, Bailey LJ, Shi XM, *et al*: Deletion of protein kinase D1 in osteoprogenitor cells results in decreased osteogenesis in vitro and reduced bone mineral density in vivo. Mol Cell Endocrinol 461: 22-31, 2018.
46. Bucay N, Sarosi I, Dunstan CR, Morony S, Tarpley J, Capparelli C, Scully S, Tan HL, Xu W, Lacey DL, *et al*: Osteoprotegerin-deficient mice develop early onset osteoporosis and arterial calcification. Genes Dev 12: 1260-1268, 1998.
47. Greenblatt MB, Shim JH, Zou W, Sitara D, Schweitzer M, Hu D, Lotinun S, Sano Y, Baron R, Park JM, *et al*: The p38 MAPK pathway is essential for skeletogenesis and bone homeostasis in mice. J Clin Invest 120: 2457-2473, 2010.
48. Jensen ED, Gopalakrishnan R and Westendorf JJ: Bone morphogenic protein 2 activates protein kinase D to regulate histone deacetylase 7 localization and repression of Runx2. J Biol Chem 284: 2225-2234, 2009.
49. Yu H, de Vos P and Ren Y: Overexpression of osteoprotegerin promotes preosteoblast differentiation to mature osteoblasts. Angle Orthod 81: 100-106, 2011.
50. Si W, Kang Q, Luu HH, Park JK, Luo Q, Song WX, Jiang W, Luo X, Li X, Yin H, *et al*: CCN1/Cyr61 is regulated by the canonical Wnt signal and plays an important role in Wnt3A-induced osteoblast differentiation of mesenchymal stem cells. Mol Cell Biol 26: 2955-2964, 2006.
51. Zhang X, Schwarz EM, Young DA, Puzas JE, Rosier RN and O'Keefe RJ: Cyclooxygenase-2 regulates mesenchymal cell differentiation into the osteoblast lineage and is critically involved in bone repair. J Clin Invest 109: 1405-1415, 2002.
52. Ford JJ, Yeh LC, Schmidgal EC, Thompson JF, Adamo ML and Lee JC: Protein kinase D1 is essential for bone acquisition during pubertal growth. Endocrinology 154: 4182-4191, 2013.
53. Yang B, Li S, Chen Z, Feng F, He L, Liu B, He T, Wang X, Chen R, Chen Z, *et al*: Amyloid β peptide promotes bone formation by regulating Wnt/β-catenin signaling and the OPG/RANKL/RANK system. FASEB J 34: 3583-3593, 2020.
54. Lacey DL, Boyle WJ, Simonet WS, Kostenuik PJ, Dougall WC, Sullivan JK, San Martin J and Dansey R: Bench to bedside: elucidation of the OPG-RANK-RANKL pathway and the development of denosumab. Nat Rev Drug Discov 11: 401-419, 2012.
55. Hoter A, El-Sabban ME and Naim HY: The HSP90 family: Structure, regulation, function, and implications in health and disease. Int J Mol Sci 19: 2560, 2018.
56. Palumbo S and Li WJ: Osteoprotegerin enhances osteogenesis of human mesenchymal stem cells. Tissue Eng Part A 19: 2176-2187, 2013.
57. Sena K, Leven RM, Mazhar K, Sumner DR and Virdi AS: Early gene response to low-intensity pulsed ultrasound in rat osteoblastic cells. Ultrasound Med Biol 31: 703-708, 2005.
58. Tabuchi Y, Hasegawa H, Suzuki N, Furusawa Y, Hirano T, Nagaoka R, Takeuchi SI, Shiiba M and Mochizuki T: Low-intensity pulsed ultrasound promotes the expression of immediate-early genes in mouse ST2 bone marrow stromal cells. J Med Ultrason (2001) 47: 193-201, 2020.
59. Veronick JA, Assanah F, Piscopo N, Kutes Y, Vyas V, Nair LS, Huey BD and Khan Y: Mechanically loading cell/hydrogel constructs with low-intensity pulsed ultrasound for bone repair. Tissue Eng Part A 24: 254-263, 2018.
60. Choudhary S, Halbout P, Alander C, Raisz L and Pilbeam C: Strontium ranelate promotes osteoblastic differentiation and mineralization of murine bone marrow stromal cells: Involvement of prostaglandins. J Bone Miner Res 22: 1002-1010, 2007.
61. Allen HL, Wase A and Bear WT: Indomethacin and aspirin: Effect of nonsteroidal anti-inflammatory agents on the rate of fracture repair in the rat. Acta Orthop Scand 51: 595-600, 1980.
62. Elmstedt E, Lindholm TS, Nilsson OS and Törnkvist H: Effect of ibuprofen on heterotopic ossification after hip replacement. Acta Orthop Scand 56: 25-27, 1985.
63. Omori K, Wada S, Maruyama Y, Hattori A, Kitamura K, Sato Y, Nara M, Funahashi H, Yachiguchi K, Hayakawa K, *et al*: Prostaglandin E2 increases both osteoblastic and osteoclastic activities in the scales of goldfish and participates in the calcium metabolism in goldfish. Zoolog Sci 29: 499-504, 2012.
64. Zuehlke AD, Beebe K, Neckers L and Prince T: Regulation and function of the human HSP90AA1 gene. Gene 570: 8-16, 2015.
65. Akerfelt M, Morimoto RI and Sistonen L: Heat shock factors: Integrators of cell stress, development and lifespan. Nat Rev Mol Cell Biol 11: 545-555, 2010.